Subduction of oceanic asthenosphere: Evidence from sub-slab seismic anisotropy

Teh-Ru Alex Song[1] and Hitoshi Kawakatsu[2]

Received 6 June 2012; revised 24 July 2012; accepted 28 July 2012; published 11 September 2012.

[1] The oceanic asthenosphere is characterized as a low viscosity channel down to 200–300 km depth separating the cold lithosphere from above, and it is intimately linked to a layer of low seismic velocity and prominent seismic anisotropy observed globally beneath ocean basins. While subduction of tectonic plates in convergent margins is well recognized, the fate of oceanic asthenosphere remains enigmatic. We demonstrate that subduction of the oceanic asthenosphere characterized by weak azimuthal anisotropy and strong radial anisotropy explains the essence of sub-slab shear-wave splitting patterns, where the fast splitting direction changes from predominantly trench-parallel (or sub-parallel) under relatively steep subduction zones to frequently trench-normal under shallow subduction zones. To explain the observed splitting time, the thickness of the subducted asthenosphere is estimated to be 100 ± 50 km. **Citation:** Song, T.-R. A., and H. Kawakatsu (2012), Subduction of oceanic asthenosphere: Evidence from sub-slab seismic anisotropy, *Geophys. Res. Lett.*, *39*, L17301, doi:10.1029/2012GL052639.

1. Introduction

[2] The nature of the oceanic asthenosphere may be understood from the perspective of mantle mineralogy [*Stixrude and Lithgow-Bertelloni*, 2005], the presence of hydrogen [*Hirth and Kohlstedt*, 1996; *Karato and Jung*, 1998] and/or the presence of a small amount of laminated melt [*Kawakatsu et al.*, 2009], which may explain the low seismic velocity, low viscosity and seismic anisotropy observed in the oceanic uppermost mantle. Such a low viscosity channel has long been envisioned as the key to long wavelength mantle convection and to maintain the long-term stability of plate tectonics [e.g., *Richards et al.*, 2001]. However, as plates subduct, it is unresolved whether the oceanic asthenosphere simply subducts along with the slab [*Ribe*, 1992] or it is decoupled from the slab involving large-scale trench-parallel flow as advocated in the past two decades [e.g., *Russo and Silver*, 1994; *Long and Silver*, 2008, 2009].

[3] Since the orientation of anisotropic mantle minerals is influenced by the direction and evolution history of the finite strain driven by mantle flows [e.g., *Becker et al.*, 2008], seismic anisotropy serves as the best proxy for the mantle deformation and flow direction. When seismic waves travel through an anisotropic medium, an incoming shear wave (S wave), bifurcates into fast and slow quasi-S waves [e.g., *Vinnik et al.*, 1984; *Babuska and Cara*, 1991], and the polarization of the two quasi-S waves is controlled by the anisotropy symmetry as well as the incoming S wave polarization direction. The S wave polarized parallel or sub-parallel to the horizontal plane is regarded as the quasi-SH wave and the other S wave as the quasi-SV wave, and we will respectively refer them as SH wave and SV wave for simplicity following the convention of seismology for a vertically stratified isotropic medium [*Aki and Richard*, 2002].

[4] To track mantle flows beneath subduction zones, we revisit the behavior of sub-slab shear wave birefringence (or splitting) compiled globally [*Long and Silver*, 2008, 2009]. We emphasize the importance of the dependence of the shear wave fast splitting direction on the seismic wave incidence angle and the slab dip, which are not taken into considerations in previous analyses. As a result, we demonstrate that observed sub-slab fast splitting directions and splitting times could be understood through the observed anisotropy property in the oceanic asthenosphere, if it subducts along with the oceanic lithosphere.

2. Sub-slab Shear Wave Splitting

[5] Sub-slab anisotropy is mostly derived from the analysis of up-going SKS wave splitting ($10° < \theta < 15°$, where θ is the incident angle) beneath seismic stations with some correction for anisotropy in the mantle wedge and the topmost subducted slab using local S wave splitting measurements [*Long and Silver*, 2008, 2009]. In some cases, downgoing teleseismic S wave, with a larger incident angle ($20° < \theta < 40°$), have also been analyzed to obtain sub-slab anisotropy beneath earthquakes (or source-side splitting) by correcting known splitting beneath the receiver [e.g., *Kaneshima and Silver*, 1992]. When local S wave splitting analysis is not available, observations at stations close to the trench are analyzed to infer sub-slab anisotropy. In principle, the effect of anisotropy in the mantle wedge and the topmost subducted slab is minimized. Since most observations and interpretations on sub-slab anisotropy are from SKS wave splitting measurements, we will primarily focus our discussion on these observations.

[6] In general, sub-slab SKS fast splitting directions are parallel or sub-parallel to the trench [*Long and Silver*, 2008, 2009] and appear distinct from the prediction of trench-normal fast splitting direction based upon the classical slab entrained flow with the A-type olivine fabric [*Karato et al.*, 2008], where the fast splitting direction manifests the flow direction. We find that these trench-parallel fast splitting

[1]Institute for Research on Earth Evolution, Japan Agency for Marine-Earth Science and Technology, Yokohama, Japan.
[2]Earthquake Research Institute, University of Tokyo, Tokyo, Japan.

Corresponding author: T.-R. A. Song, Institute for Research on Earth Evolution, Japan Agency for Marine-Earth Science and Technology, 3173-25 Showa-Machi, Yokohama 237-0005, Japan. (tehrusong@gmail.com)

0094-8276/12/2012GL052639

direction observations are typically associated with steep subduction zones (δ > 30–40°, where δ is the slab dip). However, studies in a few shallow subduction zones (δ < 20°) such as Cascadia [*Currie et al.*, 2004], Mexico [*Stubalio and Davis*, 2007], south-central Chile (S. P. Hicks et al., Sub-slab mantle anisotropy beneath south-central Chile, submitted to *Earth and Planetary Science Letters*, 2012) and Alaska [*Christensen and Abers*, 2010] show that the fast polarization direction of SKS splitting measurements at stations close to the trench is typically normal or sub-normal to the trench when incident waves travel on paths that point away from the slab dip (i.e., up-dip direction), and thus is similar to predictions from the classical slab-entrained flow. When splitting measurements from incident waves traveling on paths that point in the direction of slab dip (i.e., down-dip direction) are available, the fast splitting direction appears varying with back-azimuth and is normal or sub-normal to the direction of the incident wave [*Christensen and Abers*, 2010; Hicks et al., submitted manuscript, 2012]. In all cases, the sub-slab SKS splitting time is estimated from 0.5 seconds to about 2 seconds [*Long and Silver*, 2008, 2009].

3. Observations of Asthenosphere Anisotropy

[7] Before inferring sub-slab flow from observations of sub-slab shear-wave splitting, it is essential to recognize the characteristics of anisotropy in the oceanic asthenosphere beneath ocean basins prior to subduction. Analyses of Rayleigh waves (θ = 90°) have shown that the oceanic asthenosphere is characterized by azimuthal S wave anisotropy [e.g., *Montagner and Tanimoto*, 1991; *Maggi et al.*, 2006] (~1–3%). In this instance, horizontally traveling SV wave (θ = 90°) is typically fastest along the current plate motion direction, which is generally supported by the analysis of near-vertical SKS waves (θ ~ 10–15°) [e.g., *Montagner et al.*, 2000; *Becker et al.*, 2012].

[8] However, it is often neglected in previous interpretations of sub-slab splitting patterns that the oceanic asthenosphere is also characterized by strong P wave and S wave radial anisotropy of a few percent (up to 7% in central Pacific) in the global scale [e.g., *Gung et al.*, 2003; *Nettles and Dziewonski*, 2008] through the classical Rayleigh wave/Love wave discrepancy (θ = 90°), where the horizontally polarized SH wave is faster than the vertically polarized SV wave (or SH > SV) [*Aki and Kaminuma*, 1963; *Babuska and Cara*, 1991]. Radial anisotropy, frequently referred as transverse isotropy, can be modeled using hexagonal anisotropy with a vertical symmetry axis. Not emphasized previously, inversion results of multiple S waves such as SS, SSS, SSSS and SSSSS [*Gaherty et al.*, 1996; *Tan and Helmberger*, 2007] also indicate strong radial anisotropy symmetry at oblique incident angles (θ ~ 40–60°). Despite constraining lateral variations of radial anisotropy can be nontrivial [*Ferreira et al.*, 2010], prominent radial anisotropy of a few percent in the oceanic asthenosphere is a robust feature [*Beghein and Trampert*, 2004] and it is imbedded even in the reference Earth model [*Dziewonski and Anderson*, 1981] and a recent global 1D model for both P wave and S wave [*Kustowski et al.*, 2008]. Since the hexagonal symmetry with a horizontal fast symmetry axis generally predicts weak radial anisotropy that is comparable or smaller than azimuthal anisotropy, we find it necessary to invoke orthorhombic symmetry with a strong radial component to properly account for seismic observations in the oceanic asthenosphere.

4. Linkage Between Asthenosphere Anisotropy and Sub-slab Shear Wave Splitting

[9] To demonstrate the effect of the anisotropy symmetry on shear wave splitting directions, we construct elastic stiffness tensors for azimuthal, radial and orthorhombic anisotropy, and use the anisotropy parameter η to describe the phase velocity upon oblique incidence [*Takeuchi and Saito*, 1972]. To be consistent with observations in the oceanic asthenosphere, azimuthal anisotropy of 2% is set with a fast symmetry axis along the x_1 axis, while radial anisotropy is set at 4% and 3% for the P wave and S wave, respectively, with a slow symmetry axis along the x_3 axis. Using the theory of the effective transverse isotropy medium [*Montagner and Nataf*, 1986], orthorhombic anisotropy is set up in a way such that effective azimuthal anisotropy and effective radial anisotropy are equal to the setup in the cases of azimuth anisotropy and radial anisotropy, respectively (see also auxiliary material).[1] As a representative value, η is set at 0.95 equal to the median value observed in the oceanic asthenosphere (η ~ 0.9–1) [*Dziewonski and Anderson*, 1981; *Beghein and Trampert*, 2004; *Kustowski et al.*, 2008] (Table S1 in Text S1).

[10] While there is no observable shear wave splitting when the S wave polarization direction is parallel to the fast/slow axis, it is informative to illustrate how the fast polarization direction varies with different type of anisotropy symmetry as a function of incident angle. Here we display phase velocities of SV and SH waves along the fast symmetry axis, or the x_1 direction (Figure 1 and Figure S1 in Text S1). For an anisotropic medium with azimuth anisotropy, the SV waves are faster than the SH waves except when they are propagating along the fast symmetry axis, or θ = 90° (Figure 1a). In this case, the fast polarization directions of incoming S waves are always parallel or sub-parallel to the fast symmetry axis, or the x_1 axis. On the other hand, for an anisotropic medium with radial anisotropy and a vertical slow symmetry axis, the polarization of the fast S wave is complicated by the strength of P wave and S wave radial anisotropy, as well as the anisotropy parameter η that defines phase velocities at oblique incident angles. We find that radial anisotropy and η consistent with observations in the oceanic asthenosphere always predict the SH wave as the fast wave for all incident angles and thus the fast polarization direction is normal to the surface projection of the propagation direction (i.e., x_1 axis) (Figure 1b). This is an important prediction that is opposite to that from azimuthal anisotropy (Figure 1a).

[11] Once observed azimuthal and radial anisotropy in the oceanic asthenosphere are properly represented with orthorhombic symmetry, we observe a classical point singularity [*Crampin*, 1991] where the phase velocity of the SH wave equals to that of the SV wave at an incident angle of about 23° (Figure 1c and Figure S2 in Text S1). The polarization of the fast wave changes from the SV wave to the SH wave across such a singularity and the velocity difference between

[1] Auxiliary materials are available in the HTML. doi:10.1029/2012GL052639.

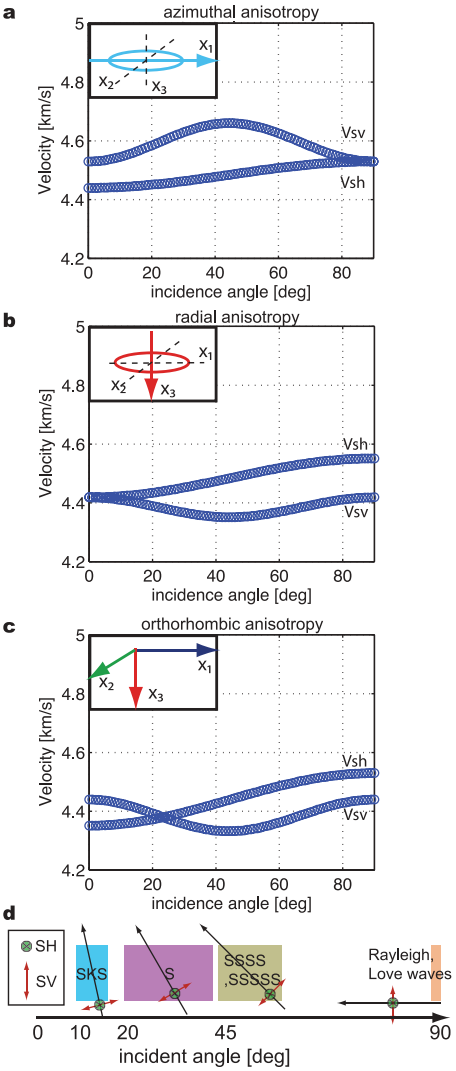

Figure 1. Phase velocities of the SV and SH waves for (a) azimuthal anisotropy, (b) radial anisotropy and (c) orthorhombic anisotropy. The result is calculated for incoming waves whose surface projection is parallel to the x_1 axis. Stereo plots including results for incoming waves from all azimuths can be referred to Figure S1 in Text S1. Note that in Figure 1c, the fast wave change from SV wave to SH wave beyond 23°, which is consistent with (d) various seismic observations at different incident angles used to constrain seismic anisotropy in the oceanic asthenosphere.

them increases with the acute angle between the incident angle and the location of the point singularity (Figure 1c). While the location of the singularity depends on the relative strength between radial anisotropy and azimuthal anisotropy as well as η [*Crampin*, 1991], we illustrate how global average of the anisotropy property in the oceanic asthenosphere dictates fast polarization directions upon different propagation directions and incident angles.

[12] These results enlighten the fact that the fast polarization direction is not necessarily parallel to the anisotropy symmetry axis, but it depends on the anisotropy symmetry as well as the direction of incoming wave and the incident angle [e.g., *Chevrot and van der Hilst*, 2003]. Although the SKS wave, a pure SV wave, is decoupled from the SH wave and is insensitive to radial anisotropy with a vertical symmetry axis, radial anisotropy with a tilted slow symmetry axis can dictate SKS wave fast splitting direction, especially at high tilted angle (>20°) [*Chevrot and van der Hilst*, 2003]. The change of the fast polarization direction as a function of incident angle shown in Figure 1c can be also used to infer the effect of slab dip for a near vertical incidence (e.g., SKS) case, assuming that the direction of symmetry axes (x_1 and x_3) rotate together with the slab dip. In such a case, the fast polarization direction switches from SV to SH as the dip angle increases. If the oceanic asthenosphere is subducting along with the slab, it is reasonable to assume that the fast symmetry axis (or the x_1 axis) is tilted parallel to the slab dip and the slow symmetry axis (or the x_3 axis) is tilted at an angle normal to the slab dip (Figures 2a–2c), a general case where the direction of absolute plate motion is normal to the trench.

[13] We illustrate equal-area stereo plots displaying predicted fast polarization directions for all propagation directions and incident angles in models with azimuthal anisotropy (Figures 2d and 2g), radial anisotropy (Figures 2e and 2h) and orthorhombic anisotropy (Figures 2f and 2i). Two cases with a slab dip of 15 degrees (Figures 2d–2f) and 40 degrees (Figures 2g–2i) are presented to demonstrate the effect of slab dip on the shear wave fast polarization direction. Regardless of the slab dip, we find that azimuthal anisotropy with a tilted fast symmetry axis predicts fast splitting direction parallel or sub-parallel to the subduction direction (x_1 axis) (Figures 2d and 2g) upon incident angle of SKS waves ($10° < \theta < 15°$), e.g., fast splitting direction is universally normal or sub-normal to the trench. On the other hand, radial anisotropy with a tilted slow symmetry axis often results in fast splitting direction oblique to the trench for shallow subduction (Figure 2e) and sub-parallel to the trench for steep subduction (Figure 2h).

[14] Orthorhombic anisotropy with a tilted symmetry axis reveals that fast splitting direction is strongly influenced by the slab dip (Figures 2f and 2i). For a slab dip of 15 degrees, the fast splitting direction is predominantly normal or sub-normal to the trench (or along x_1 axis) in the up-dip direction (Figure 2f). The predicted splitting time is generally very small for the near-vertical SKS wave from the down-dip direction, but the fast splitting direction appears normal or sub-normal to the direction of the incoming wave. We find these predictions generally consistent with sub-slab SKS fast splitting direction observed near the trench in shallow subduction zones [*Currie et al.*, 2004; *Stubalio and Davis*, 2007; Hicks et al., submitted manuscript, 2012]. For a sub-horizontal slab ($\delta < 10°$), the SKS fast splitting direction is always normal or sub-normal to the trench [*Christensen and Abers*, 2010] (see also Figure S1c in Text S1).

[15] For a slab dip of 40 degrees, the fast splitting direction is predominantly parallel or sub-parallel to the trench (or x_2 axis) and it does not vary substantially with ray back-azimuth (Figure 2i). This prediction is consistent with observations of the so-called trench-parallel splitting observations in most of the subduction zones [13 out of 15 in *Long and Silver*, 2009]. In these cases, the change of fast splitting direction is controlled by the acute angle between the tilted slow symmetry axis and the incident wave as well as the location of point singularity, which is demonstrated in Figure 1c. Finally, we note that our result does not depend on the particular choice of anisotropy parameters presented

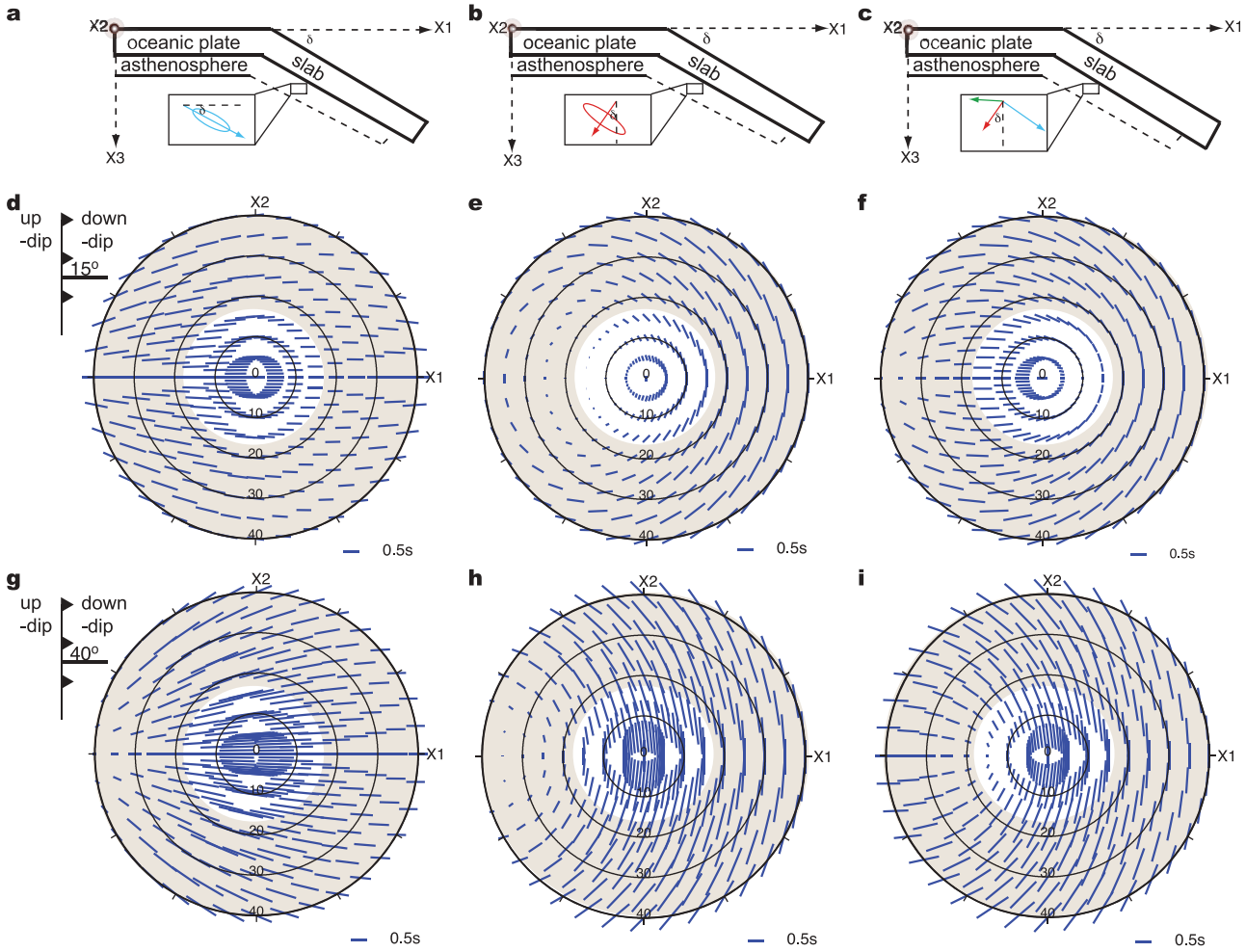

Figure 2. Stereo plots of fast polarization directions upon different type of anisotropy symmetry and slab dip. X_1 and X_2 represent the direction of fast axis and the orientation of the trench, respectively. The direction of the bar represents the polarization of the fast wave projected on the horizontal plane (or X_1–X_2 plane) at a given back azimuth and incident angle and its length indicates the arrival time difference between the fast wave and slow wave, equivalently the splitting time. (a–c) The model geometry with azimuthal anisotropy, radial anisotropy and orthorhombic anisotropy in the subducted oceanic asthenosphere, respectively. (d–f) Fast polarization directions predicted for a slab dip of 15° and anisotropy symmetry shown in Figures 2a–2c, respectively. (g–i) Fast polarization directions predicted for a slab dip of 40° and anisotropy symmetry shown in Figures 2a–2c, respectively. Incident angles of the SKS wave and the S wave are shown in white and light brown regime, respectively. The strength of azimuthal anisotropy, radial anisotropy and η are the same as those in Figure 1.

here and the conclusion remains over a wide range of parameters that satisfy observations in the oceanic asthenosphere (Figure S2 in Text S1).

5. Discussions and Conclusions

[16] These results indicates that the orthorhombic anisotropy that is consistent with the observed seismic properties of the oceanic asthenosphere (including surface waves) may explain the observations of sub-slab SKS splitting pattern, if the oceanic asthenosphere subducts along with the slab. We thus infer that the orientation of the sub-slab SKS fast splitting direction is predominantly controlled by the nature of anisotropy already in the oceanic asthenosphere and the dipping angle of the slab. In the instances where the incoming plate motion is oblique to the trench (see also auxiliary material), the SKS splitting pattern is rotated with respect to the incoming plate motion direction in shallow subduction zones (Figure S3 in Text S1), but remains parallel or sub-parallel to the trench at steep subduction zones since it is dominated by the effect of strong radial anisotropy through the slab dip (Figure S3 in Text S1).

[17] To estimate the thickness of the entrained oceanic asthenosphere globally, we calculate synthetic waveform and compute SKS splitting times for various slab dips (see also auxiliary material, Figure S4 in Text S1). To obtain a first order estimate, we assume that the motion of the incoming plate is normal to the trench for all cases with a complete azimuthal coverage (see auxiliary material and Figure S5 in Text S1). In general, the thickness of subducted oceanic asthenosphere is about 100 $\pm$ 50 km and it reproduces sub-slab SKS splitting times of 0.5–2 seconds observed in global subduction zones (Figure 3). The thickness in the southwest Pacific (Tonga-Kermadec, New Zealand) appears thinner than that beneath the young plates in the eastern Pacific (Cascadia, South America, Middle America),

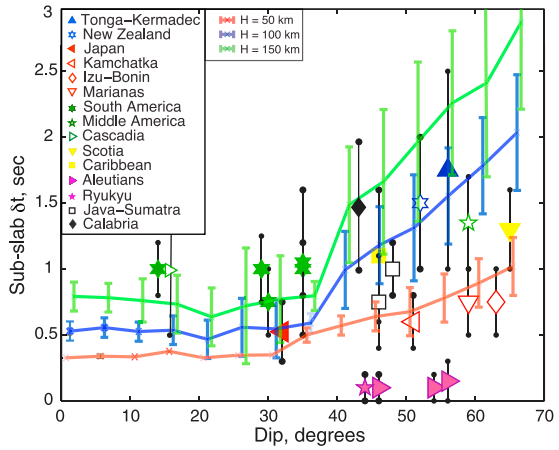

Figure 3. Thickness of the subducted oceanic asthenosphere. Global sub-slab splitting times [after *Long and Silver*, 2009] are plotted against slab dip with the predicted splitting time of asthenosphere thickness H = 50, 100, 150 km. Assuming an incident angle of 12.5°, synthetic splitting times are computed with the orthorhombic anisotropy symmetry following the modeling geometry depicted in Figure 2a and presented with their arithmetic means and standard deviations (see also auxiliary material), which are indicative of the amplitude of azimuthal variation in splitting times (Figure S4 in Text S1). The predicted fast splitting directions change from predominantly trench-normal at shallow subduction to predominantly trench-parallel at steep subduction (Figure S4 in Text S1).

but thicker than that beneath the old plates in the northwestern Pacific (Japan, Kamchatka, Izu-Bonin, Mariana). It is, however, premature to precisely estimate the thickness of subducted asthenosphere without high-resolution regional anisotropic model beneath the incoming plate for different subduction zones, but it appears difficult to argue against subduction of oceanic asthenosphere itself.

[18] As noted by *Long and Silver* [2008, 2009], Aleutians and Ryukyu subduction zones show minimum splitting time (~0.3 seconds or less). Since sub-slab splitting is dictated by the anisotropy property of the oceanic asthenosphere beneath the incoming plate, one sensible interpretation in the context of asthenosphere subduction is that the asthenosphere anisotropy property of the incoming plate may be significantly different from the global average, which can influence splitting time as well as splitting direction (Figure S6 in Text S1). Another possibility is that the strong anisotropy in the wedge above the slab may make it difficult to see sub-slab anisotropy from SKS splitting.

[19] We conclude that asthenosphere subduction is substantial (~100 ± 50 km thick) on a global scale, supporting a significant coupling between the subducting slab and the oceanic asthenosphere, and potentially defying strong buoyancy associated with the oceanic asthenosphere for limited entrainment [e.g., *Phipps Morgan et al.*, 2007; *Long and Silver*, 2009]. This result also provides a new perspective on the nature of the oceanic asthenosphere. While any of the olivine fabrics (A, D, E-type with slip in a-axis direction) will show radial anisotropy for a horizontal flow [*Mainprice*, 2007; *Karato et al.*, 2008], the strength of radial component is comparably weaker than the azimuthal anisotropy and inconsistent with seismic observations. The presence of horizontal melt layer could boost the strength of radial anisotropy [*Mainprice*, 1997; *Kawakatsu et al.*, 2009]. However, as the oceanic asthenosphere subducts along with the subducting slab, any melt that may be present is likely solidified, which significantly reduces the strength of radial anisotropy. To maintain the anisotropy property in the oceanic asthenosphere during subduction, the background solid fabric must also display orthorhombic symmetry with a strong radial component, which may be influenced by the greater pyroxene content prior to melting [*Mainprice and Silver*, 1993], oriented melt pockets [e.g., *Holtzman et al.*, 2003; *Holtzman and Kendall*, 2010], simultaneous activation of different slip systems [e.g., *Ohuchi et al.*, 2011] or/and transpression deformation [e.g., *Tommasi et al.*, 1999].

[20] In any case, if subduction of the oceanic asthenosphere (~100 ± 50 km) is continuing down to the deep upper mantle, as inferred from this study, the mass flux and geochemical mixing associated with the entrained mantle via subduction may have been underestimated and deserve to be revisited. Future examination and validation of global asthenosphere subduction against other hypotheses [*Russo and Silver*, 1994; *Long and Silver*, 2008; *Faccenda et al.*, 2008; *Jung et al.*, 2009] can be done by examining splitting measurements from oblique incident teleseismic S waves ($20° < \theta < 40°$), which are expected to display considerable azimuthal variation in the fast splitting direction and sometimes differ from SKS splitting measurements (Figure 2). This will be an important and immediate subject for the future research. In addition, the linkage between surface wave azimuthal anisotropy and SKS splitting in subduction zones may be generalized from the assumption of a horizontal fast symmetry axis [*Montagner et al.*, 2000] to a tilted slow symmetry axis or more general orthorhombic symmetry. Last but not least, the simultaneous analysis of in-situ OBS observation data for the surface wave dispersion and the shear wave splitting will undoubtedly help to better constrain the relative strength between azimuthal and radial anisotropy and to further verify the basis of our inference.

[21] **Acknowledgments.** We thank A. Federiksen and M. Bostock for providing software for calculating shear wave splitting functions for dipping anisotropic layers. TAS greatly thanks support by D. Suetsugu (IFREE) and M. Bostock (UBC) for the summer visit in 2011. We greatly benefit from discussions with L.-J. Liu, M. Bostock and N. Christensen during the course of this study. We thank D. Anderson for his review in the early draft and Y. Fukao, L. Stixrude and C. Lithgow-Bertelloni for discussions. This study is supported by IFREE, JAMSTEC (TAS), and partly supported by Grant-in-Aid for Scientific Research 22000003 granted to ERI (HK) through the JSPS. Comments from two anonymous reviewers help clarify our paper.

[22] The Editor thanks two anonymous reviewers for assisting in the evaluation of this paper.

References

Aki, K., and K. Kaminuma (1963), Phase velocity of Love waves in Japan, part I: Love waves from Aleutian shock of March 9, 1957, *Bull. Earth. Res. Inst. Univ. Tokyo*, *41*, 243–259.

Aki, K., and P. G. Richard (2002), *Quantitative Seismology*, 2nd ed, Univ. Sci., Sausalito, Calif.

Babuska, V., and M. Cara (1991), *Seismic Anisotropy in the Earth*, Kluwer Acad., Boston, Mass.

Becker, T. W., B. Kustowski, and G. Ekström (2008), Radial seismic anisotropy as a constraint for upper mantle rheology, *Earth Planet. Sci. Lett.*, *267*, 213–227, doi:10.1016/j.epsl.2007.11.038.

Becker, T. W., S. Lebedev, and M. Long (2012), On the relationship between azimuthal anisotropy from shear wave splitting and surface

wave tomography, *J. Geophys. Res.*, *117*, B01306, doi:10.1029/2011JB008705.
Beghein, C., and J. Trampert (2004), Probability density functions for radial anisotropy from fundamental surface wave data and the Neighbourhood algorithm, *Geophys. J. Int.*, *157*, 1163–1174, doi:10.1111/j.1365-246X.2004.02235.x.
Chevrot, S., and R. D. van der Hilst (2003), On the effect of a dipping axis of symmetry on shear wave splitting measurements in a transversely isotropic medium, *Geophys. J. Int.*, *152*, 497–505, doi:10.1046/j.1365-246X.2003.01865.x.
Christensen, D. H., and G. Abers (2010), Seismic anisotropy under central Alaska from SKS splitting observations, *J. Geophys. Res.*, *115*, B04315, doi:10.1029/2009JB006712.
Crampin, S. (1991), Effect of point singularities on shear-wave propagation in sedimentary basins, *Geophys. J. Int.*, *107*, 531–543, doi:10.1111/j.1365-246X.1991.tb01413.x.
Currie, C. A., J. F. Cassidy, R. F. Hyndman, and M. G. Bostock (2004), Shear wave anisotropy beneath the Cascadia subduction zone and western North America, *Geophys. J. Int.*, *157*, 341–353, doi:10.1111/j.1365-246X.2004.02175.x.
Dziewonski, A. D., and D. L. Anderson (1981), Preliminary reference Earth model, *Phys. Earth Planet. Inter.*, *25*, 297–356, doi:10.1016/0031-9201(81)90046-7.
Faccenda, M., L. Burlin, T. V. Gerya, and D. Mainprice (2008), Fault-induced seismic anisotropy by hydration in subducting oceanic plates, *Nature*, *455*, 1097–1100, doi:10.1038/nature07376.
Ferreira, A. M., A. Woodhouse, K. Kisser, and J. Trampert (2010), On the robustness of globally radial anisotropic surface wave tomography, *J. Geophys. Res.*, *115*, B04313, doi:10.1029/2009JB006716.
Gaherty, J. B., T. H. Jordan, and L. S. Goes (1996), Seismic structure of the upper mantle in a central Pacific corridor, *J. Geophys. Res.*, *101*, 22,291–22,309, doi:10.1029/96JB01882.
Gung, Y., M. Panning, and B. Romanowicz (2003), Global anisotropy and the thickness of continent, *Nature*, *422*, 707–711, doi:10.1038/nature01559.
Hirth, G., and D. L. Kohlstedt (1996), Water in the oceanic upper mantle: implications for rheology, melt extraction and the evolution of the lithosphere, *Earth Planet. Sci. Lett.*, *144*, 93–108, doi:10.1016/0012-821X(96)00154-9.
Holtzman, B. K., and J.-M. Kendall (2010), Organized melt, seismic anisotropy, and plate boundary lubrication, *Geochem. Geophys. Geosyst.*, *11*, Q0AB06, doi:10.1029/2010GC003296.
Holtzman, B. K., D. Kohlstedt, M. Zimmerman, F. Heidelbach, T. Hiraga, and J. Hustoft (2003), Melt segregation and strain partitioning: Implications for seismic anisotropy and mantle flow, *Science*, *301*, 1227–1230, doi:10.1126/science.1087132.
Jung, H., W. Mo, and H. W. Green (2009), Upper mantle seismic anisotropy resulting from pressure-induced slip transition in olivine, *Nat. Geosci.*, *2*, 73–77, doi:10.1038/ngeo389.
Kaneshima, S., and P. G. Silver (1992), A search for source side mantle anisotropy, *Geophys. Res. Lett.*, *19*, 1049–1052, doi:10.1029/92GL00899.
Karato, S. I., and H. Jung (1998), Water, partial melting and the origin of the seismic low velocity and high attenuation zone in the upper mantle, *Earth Planet. Sci. Lett.*, *157*, 193–207, doi:10.1016/S0012-821X(98)00034-X.
Karato, S.-I., H. Jung, I. Katayama, and P. Skemer (2008), Geodynamic signatures of seismic anisotropy of the upper mantle: New insights from laboratory studies, *Annu. Rev. Earth Planet. Sci.*, *36*, 59–95, doi:10.1146/annurev.earth.36.031207.124120.
Kawakatsu, H., P. Kumar, Y. Takei, M. Shinohara, T. Kanazawa, E. Araki, and K. Suyehiro (2009), Seismic evidence for sharp lithosphere-asthenosphere boundaries of oceanic plates, *Science*, *324*, 499–502, doi:10.1126/science.1169499.
Kustowski, B., G. Ekström, and A. M. Dziewonski (2008), Anisotropic shear-wave velocity structure of the Earth's mantle: A global model, *J. Geophys. Res.*, *113*, B06306, doi:10.1029/2007JB005169.
Long, M., and P. G. Silver (2008), The subduction zone flow field from seismic anisotropy: A global view, *Science*, *319*, 315–318, doi:10.1126/science.1150809.
Long, M., and P. G. Silver (2009), Mantle flow in subduction systems: The subslab flow field and implications for mantle dynamics, *J. Geophys. Res.*, *114*, B10312, doi:10.1029/2008JB006200.
Maggi, A., E. Debayle, K. Priestley, and G. Barruol (2006), Azimuthal anisotropy of the Pacific region, *Earth Planet. Sci. Lett.*, *250*, 53–71, doi:10.1016/j.epsl.2006.07.010.
Mainprice, D. (1997), Modelling the anisotropic seismic properties of partially molten rocks found at mid-ocean ridges, *Tectonophysics*, *279*, 161–179, doi:10.1016/S0040-1951(97)00122-4.
Mainprice, D. (2007), Seismic anisotropy of the deep Earth from a mineral and rock physics perspectives, in *Treatise on Geophysics*, vol. 2, *Mineral Physics*, edited by G. Schubert, pp. 437–491, Elsevier, Amsterdam, doi:10.1016/B978-044452748-6/00045-6.
Mainprice, D., and P. G. Silver (1993), Interpretations of SKS waves using samples from subcontinental lithosphere, *Phys. Earth Planet. Inter.*, *78*, 257–280, doi:10.1016/0031-9201(93)90160-B.
Montagner, J.-P., and H.-C. Nataf (1986), A simple method for inverting the azimuthal anisotropy of surface wave, *J. Geophys. Res.*, *91*, 511–520, doi:10.1029/JB091iB01p00511.
Montagner, J. P., and T. Tanimoto (1991), Global upper mantle tomography of seismic velocities and anisotropy, *J. Geophys. Res.*, *96*, 20,337–20,351, doi:10.1029/91JB01890.
Montagner, J.-P., D.-A. Griot-Pommera, and J. Lave (2000), How to relate body wave and surface wave anisotropy, *J. Geophys. Res.*, *105*, 19,015–19,027, doi:10.1029/2000JB900015.
Nettles, M., and A. M. Dziewonski (2008), Radially anisotropic shear velocity structure of the upper mantle globally and beneath North America, *J. Geophys. Res.*, *113*, B02303, doi:10.1029/2006JB004819.
Ohuchi, T., T. Kawazoe, Y. Nishihara, N. Nishiyama, and T. Irifune (2011), High pressure and temperature fabric transitions in olivine and variations in upper mantle seismic anisotropy, *Earth Planet. Sci. Lett.*, *304*, 55–63, doi:10.1016/j.epsl.2011.01.015.
Phipps Morgan, J., J. Hasenclever, M. Hort, L. Rupke, and E. M. Parmentier (2007), On subducting slab entrainment of buoyant asthenosphere, *Terra Nova*, *19*, 167–173, doi:10.1111/j.1365-3121.2007.00737.x.
Ribe, M. (1992), On the relation between seismic anisotropy and finite strain, *J. Geophys. Res.*, *97*, 8737–8747, doi:10.1029/92JB00551.
Richards, M. A., W.-S. Yang, J. R. Baumgardner, and H.-P. Bunge (2001), Role of low-viscosity zone in stabilizing plate tectonics: Implications for comparative terrestrial planetology, *Geochem. Geophys. Geosyst.*, *2*, 1026, doi:10.1029/2000GC000115.
Russo, R. M., and P. G. Silver (1994), Trench-parallel flow beneath the Nazca plate from seismic anisotropy, *Science*, *263*, 1105–1111, doi:10.1126/science.263.5150.1105.
Stixrude, L., and C. Lithgow-Bertelloni (2005), Mineralogy and elasticity of the oceanic upper mantle: Origin of the low-velocity zone, *J. Geophys. Res.*, *110*, B03204, doi:10.1029/2004JB002965.
Stubalio, I., and P. Davis (2007), Shear wave splitting measurements and interpretation beneath Acapulco-Tampico transect, *Eos Trans. AGU*, *88*(52), Fall Meet Suppl., Abstract T51B-0539.
Takeuchi, H., and M. Saito (1972), Seismic surface waves, *Methods Comput. Phys.*, *11*, 217–295.
Tan, Y., and D. V. Helmberger (2007), Trans-Pacific upper mantle shear velocity structure, *J. Geophys. Res.*, *112*, B08301, doi:10.1029/2006JB004853.
Tommasi, A., B. Tikoff, and A. Vauchez (1999), Upper mantle tectonics: Three-dimensional deformation, olivine crystallographic fabrics and seismic properties, *Earth Planet. Sci. Lett.*, *168*, 173–186, doi:10.1016/S0012-821X(99)00046-1.
Vinnik, L. P., G. L. Kosarev, and L. I. Makeyeva (1984), Anisotropiy litosfery ponablyudeniyam voln SKS and SKKS, *Dok. Akad. Nauk USSR.*, *278*, 1335–1339.